In-phase and antiphase dynamics of Rydberg atoms with distinguishable resonances

Chu-Hui Fan,[1,2] Han-Xiao Zhang,[1,2] and Jin-Hui Wu[1,2,*]

[1]*Center for Quantum Sciences, Northeast Normal University, Changchun 130117, People's Republic of China*

[2]*School of Physics, Northeast Normal University, Changchun 130024, People's Republic of China*

(Received 18 November 2018; published 6 March 2019)

We study the correlated evolutions of two Rydberg atoms, interacting via a van der Waals (vdW) potential V_6 and driven by a laser field of detunings Δ_1 and Δ_2. The two atoms may exhibit the in-phase dynamics with identical Rydberg populations or the antiphase dynamics with complementary Rydberg populations, depending on their initial states. For a moderate vdW potential far from the blockade regime, the in-phase or antiphase dynamics can be attained along two intersecting lines in the parameter space of Δ_1 and Δ_2 with an *exact* or *approximate* figure of merit, respectively. Note, in particular, that the *exact* in-phase dynamics is *trivial* because it requires identical detunings while the *approximate* in-phase, *exact* antiphase, and *approximate* antiphase dynamics are *nontrivial* because they require distinct detunings. The specific requirements on Δ_1 and Δ_2 for both in-phase and antiphase dynamics can be understood by considering the balanced transitions from two initially populated states to two initially empty states in the double-atom state basis.

DOI: 10.1103/PhysRevA.99.033813

I. INTRODUCTION

Rydberg atoms have many interesting features, one of which is the long-range dipole-dipole interaction (DDI), usually manifested as a van der Waals (vdW) potential. The vdW potential may induce a large resonance shift for a double Rydberg excitation so that the excitation of one Rydberg atom strictly suppresses the excitation of another Rydberg atom, yielding then the so-called blockade effect [1–3]. But it is also viable to realize the simultaneous excitation of two Rydberg atoms by compensating the vdW induced resonance shift with a suitable atom-light detuning, which is usually referred to as the antiblockade effect [4–6]. With the blockade or antiblockade effect, Rydberg atoms have been proven to be a promising platform for implementing many quantum tasks [1] to realize, e.g., diverse quantum entanglement [7–11], efficient quantum gates [12–16], photonic devices [17–21], and deterministic single-photon sources [22–25].

Note, in particular, that a cooperative absorptive nonlinearity has been found for Rydberg atomic ensembles in the regime of electromagnetically induced transparency (EIT), manifested as the output spectra of a probe field sensitive to its input intensity [26–29]. More importantly, the output probe photons may exhibit strong repulsive interactions, as they suffer a largely modified statistics of remarkable antibunching features. This allows the realization of a nonlinear EIT medium transparent to single photons but opaque to multiple photons, and has aroused great interest in developing theories on single-photon propagation dynamics [30–33]. The cooperative nonlinearity for Rydberg atomic ensembles will turn from absorptive to dispersive if one works inside an EIT window of very large atom-light detunings [34]. This then yields the attractive single-photon interactions constituting the basis of two-photon and three-photon bound states [35–37]. The repulsive (absorptive) or attractive (dispersive) interactions (nonlinearities), as a long-standing goal in quantum photonics, enable usually unavailable applications in quantum information science like single-photon gates [38–40] and memories [41–43].

On the other hand, benefiting from the fast development of experimental technologies, we now can capture single atoms in optical microtraps and arrange them to one-dimensional (1D) chains or two-dimensional (2D) arrays. Such Rydberg atomic structures may serve as an alternative platform different from Rydberg atomic ensembles for implementing various quantum tasks, including the realization of quantum gates in terms of atomic qubits [44–49] and the simulation of spin dynamics in terms of excitation transport [50–53]. In addition, the 1D Rydberg chains or 2D Rydberg arrays have been explored to examine nonequilibrium phase transitions [54], magnetization quantum revivals [55], correlated population oscillations [56], etc. In most of the above studies and other relevant works [57–60], dynamic evolutions of collective Rydberg excitations are inevitably considered as the direct or indirect evidences of concerned issues for a given vdW potential. But it is not clear yet how Rydberg atoms transit from the completely independent to the strongly correlated oscillations as the vdW potential gradually increases until entering the blockade regime.

Here we consider two Rydberg atoms of different atom-light detunings Δ_1 and Δ_2 to examine their correlated evolutions in the presence of a vdW potential V_6. Our numerical results show that they can exhibit the in-phase dynamics referring to identical Rydberg populations and the antiphase dynamics referring to complementary Rydberg populations for different initial states. These are attained at the middle stage as the vdW potential is increased to result in the continuous transitions of complete independence – weak correlation – moderate correlation – strong correlation – rigid blockade.

*jhwu@nenu.edu.cn

To be more specific, the realization of exact (approximate) in-phase dynamics requires $\Delta_1 = \Delta_2$ ($\Delta_1 + \Delta_2 = 3V_6/2$) while the realization of exact (approximate) antiphase dynamics requires $\Delta_1 + \Delta_2 = V_6$ ($\Delta_1 - \Delta_2 = V_6/2$). These requirements reflect the fact that two initially empty states in the double-atom state basis should remain equal populations, which can only be attained when they have identical or opposite detunings to two initially populated states. Finally, we stress that our findings can be extended to design reliable schemes for implementing the dynamic control of atomic entanglement, e.g., by considering two pairs of closely lying Rydberg atoms. In this case, it is viable to attain a high-fidelity entangled state $(|gr\rangle + |rg\rangle)/\sqrt{2}[(|gg\rangle - |rr\rangle)/\sqrt{2}]$, far from the blockade regime, by exploring the antiphase (in-phase) dynamics.

II. MODEL AND EQUATIONS

We consider in Fig. 1 a pair of two-level atoms loaded into different optical traps with the ground states $|g_{1,2}\rangle$ and the Rydberg states $|r_{1,2}\rangle$. They are assumed to be driven by a common laser field of frequency ω_d and amplitude E_d in the presence of different transition frequencies $\omega_{1,2}$. They also interact through a van der Waals (vdW) potential $V_6 = C_6/R_{12}^6$ with C_6 being the vdW coefficient and R_{12} the interatomic distance. Then, with the rotating-wave and electric-dipole approximations, we can write down the the total Hamiltonian

$$\mathcal{H} = \hbar \begin{pmatrix} 0 & \Omega_2^* & \Omega_1^* & 0 \\ \Omega_2 & \Delta_2 & 0 & \Omega_1^* \\ \Omega_1 & 0 & \Delta_1 & \Omega_2^* \\ 0 & \Omega_1 & \Omega_2 & \Delta_1 + \Delta_2 - V_6 \end{pmatrix}, \tag{1}$$

in the double-atom state basis of $|g_1g_2\rangle$, $|g_1r_2\rangle$, $|r_1g_2\rangle$, and $|r_1r_2\rangle$. In Eq. (1), we have defined $\Delta_{1,2} = \omega_d - \omega_{1,2}$ as detunings and $\Omega_{1,2} = E_d d_{1,2}/2\hbar$ as Rabi frequencies, accounting for the near-resonant interactions between the driving field and both Rydberg atoms, with $d_{1,2}$ being the electric dipole moments on relevant transitions.

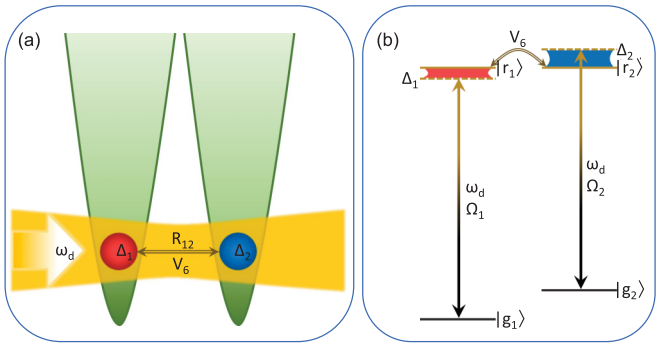

FIG. 1. (a) Two Rydberg atoms loaded into different traps of distance R_{12}, coupled via a vdW interaction of potential V_6, and driven by a common laser of frequency ω_d. (b) The corresponding level configuration with ground states $|g_j\rangle$ and Rydberg states $|r_j\rangle$ coupled by the common laser of detunings Δ_j and Rabi frequencies Ω_j. The vdW interaction can result in the in-phase and antiphase dynamics for different initial conditions.

The dynamics of one atomic system is governed by the master equation for density operator ρ

$$\partial_t \rho = -\frac{i}{\hbar}[\mathcal{H}, \rho] + \mathcal{L}(\rho), \tag{2}$$

with $\mathcal{L}(\rho) = \sum_j \Gamma_j[\sigma_{gr_j}\rho\sigma_{r_jg} - \frac{1}{2}(\rho\sigma_{r_jg}\sigma_{gr_j} + \sigma_{r_jg}\sigma_{gr_j}\rho)]$ describing the dissipation processes arising from the Rydberg decay rates Γ_j, where $\sigma_{r_jg} = |r_j\rangle\langle g|$ and $\sigma_{gr_j} = |g\rangle\langle r_j|$ have been introduced to represent the raising and lowering operators for relevant transitions. Using the total Hamiltonian $\mathcal{H}$, it is straightforward to expand Eq. (2) into the following density matrix equations:

$$\begin{aligned}
\partial_t \rho_{g_1g_1,g_2g_2} &= +\Gamma_1\rho_{r_1r_1,g_2g_2} + \Gamma_2\rho_{g_1g_1,r_2r_2} - i\big(\Omega_1\rho_{g_1r_1,g_2g_2} - \Omega_1^*\rho_{r_1g_1,g_2g_2}\big) - i\big(\Omega_2\rho_{g_1g_1,g_2r_2} - \Omega_2^*\rho_{g_1g_1,r_2g_2}\big),\\
\partial_t \rho_{g_1g_1,r_2r_2} &= +\Gamma_1\rho_{r_1r_1,r_2r_2} - \Gamma_2\rho_{g_1g_1,r_2r_2} - i\big(\Omega_1\rho_{g_1r_1,r_2r_2} - \Omega_1^*\rho_{r_1g_1,r_2r_2}\big) + i\big(\Omega_2\rho_{g_1g_1,g_2r_2} - \Omega_2^*\rho_{g_1g_1,r_2g_2}\big),\\
\partial_t \rho_{r_1r_1,g_2g_2} &= +\Gamma_2\rho_{r_1r_1,r_2r_2} - \Gamma_1\rho_{r_1r_1,g_2g_2} + i\big(\Omega_1\rho_{g_1r_1,g_2g_2} - \Omega_1^*\rho_{r_1g_1,g_2g_2}\big) - i\big(\Omega_2\rho_{r_1r_1,g_2r_2} - \Omega_2^*\rho_{r_1r_1,r_2g_2}\big),\\
\partial_t \rho_{g_1r_1,g_2g_2} &= -(i\Delta_1 + \Gamma_1/2)\rho_{g_1r_1,g_2g_2} + \Gamma_2\rho_{g_1r_1,r_2r_2} - i\big(\Omega_2\rho_{g_1r_1,g_2r_2} - \Omega_2^*\rho_{g_1r_1,r_2g_2}\big) + i\Omega_1^*\big(\rho_{r_1r_1,g_2g_2} - \rho_{g_1g_1,g_2g_2}\big),\\
\partial_t \rho_{g_1g_1,g_2r_2} &= -(i\Delta_2 + \Gamma_2/2)\rho_{g_1g_1,g_2r_2} + \Gamma_1\rho_{r_1r_1,g_2r_2} - i\big(\Omega_1\rho_{g_1r_1,g_2r_2} - \Omega_1^*\rho_{r_1g_1,g_2r_2}\big) + i\Omega_2^*\big(\rho_{g_1g_1,r_2r_2} - \rho_{g_1g_1,g_2g_2}\big),\\
\partial_t \rho_{g_1r_1,r_2g_2} &= -[i(\Delta_1 - \Delta_2) - (\Gamma_1 + \Gamma_2)/2]\rho_{g_1r_1,r_2g_2} - i\Omega_1^*\big(\rho_{g_1g_1,r_2g_2} - \rho_{r_1r_1,r_2g_2}\big) - i\Omega_2\big(\rho_{g_1r_1,r_2r_2} - \rho_{g_1r_1,g_2g_2}\big),\\
\partial_t \rho_{g_1r_1,g_2r_2} &= -[i(\Delta_1 + \Delta_2 - V_6) + (\Gamma_1 + \Gamma_2)/2]\rho_{g_1r_1,g_2r_2} - i\Omega_1^*\big(\rho_{g_1g_1,g_2r_2} - \rho_{r_1r_1,g_2r_2}\big) + i\Omega_2^*\big(\rho_{g_1r_1,r_2r_2} - \rho_{g_1r_1,g_2g_2}\big),\\
\partial_t \rho_{g_1r_1,r_2r_2} &= -[i(\Delta_1 - V_6) + (\Gamma_1/2 + \Gamma_2)]\rho_{g_1r_1,r_2r_2} + i\big(\Omega_2\rho_{g_1r_1,g_2r_2} - \Omega_2^*\rho_{g_1r_1,r_2g_2}\big) + i\Omega_1^*\big(\rho_{r_1r_1,r_2r_2} - \rho_{g_1g_1,r_2r_2}\big),\\
\partial_t \rho_{r_1r_1,g_2r_2} &= -[i(\Delta_2 - V_6) + (\Gamma_2/2 + \Gamma_1)]\rho_{r_1r_1,g_2r_2} + i\big(\Omega_1\rho_{g_1r_1,g_2r_2} - \Omega_1^*\rho_{r_1g_1,g_2r_2}\big) + i\Omega_2^*\big(\rho_{r_1r_1,r_2r_2} - \rho_{r_1r_1,g_2g_2}\big),
\end{aligned} \tag{3}$$

constrained by $\sum_{ik}\rho_{ii,kk} = 1$, $\rho_{ii,kl} = \rho_{ii,lk}^*$, $\rho_{ij,kk} = \rho_{ji,kk}^*$, and $\rho_{ij,kl} = \rho_{ji,lk}^*$ with $\{i, j\} \in \{g_1, r_1\}$ for the first Rydberg atom and $\{k, l\} \in \{g_2, r_2\}$ for the second Rydberg atom. Then we can solve Eq. (3) with a certain initial condition [e.g., $\rho_{g_1g_1,g_2g_2}(0) = 1$ or $\rho_{g_1g_1,r_2r_2}(0) = 1$] to calculate the reduced density matrices $\rho_1 = \mathrm{Tr}_2(\rho)$ and $\rho_2 = \mathrm{Tr}_1(\rho)$. This allows us to examine whether the two Rydberg atoms of different resonant frequencies $\omega_{1,2}$ (driving detunings $\Delta_{1,2}$) can exhibit the in-phase [characterized by $\rho_{r_1r_1}(t) = \rho_{r_2r_2}(t)$ and $\rho_{g_1r_1}(t) = \rho_{g_2r_2}(t)$] or the antiphase [characterized by $\rho_{r_1r_1}(t) = \rho_{g_2g_2}(t)$ and $\rho_{g_1r_1}(t) = \rho_{r_2g_2}(t)$] dynamics, in the presence of an appropriate vdW potential V_6. It is also easy to see that V_6 appears only in the last three rows in Eq. (3), which account for one double-photon transition ($|g_1g_2\rangle \to |r_1r_2\rangle$) and two

single-photon transitions ($|g_1r_2\rangle \to |r_1r_2\rangle$ and $|r_1g_2\rangle \to |r_1r_2\rangle$) of the same final state.

Note, however, that incorrect results will be attained if we change the order of solving density matrix equations and making partial traces as mentioned above. That is, it is not logical if we first attain from Eq. (3)

$$\begin{aligned}
\partial_t \rho_{r_1r_1} &= -\Gamma_1 \rho_{r_1r_1} + i\big(\Omega_1 \rho_{g_1r_1} - \Omega_1^* \rho_{r_1g_1}\big),\\
\partial_t \rho_{g_1r_1} &= -[i(\Delta_1 - V_6) + \Gamma_1/2]\rho_{g_1r_1}\\
&\quad + i\Omega_1^*\big(\rho_{r_1r_1} - \rho_{g_1g_1}\big),\\
\partial_t \rho_{r_2r_2} &= -\Gamma_2 \rho_{r_2r_2} + i\big(\Omega_2 \rho_{g_2r_2} - \Omega_2^* \rho_{r_2g_2}\big),\\
\partial_t \rho_{g_2r_2} &= -[i(\Delta_2 - V_6) + \Gamma_2/2]\rho_{g_2r_2}\\
&\quad + i\Omega_2^*\big(\rho_{r_2r_2} - \rho_{g_2g_2}\big),
\end{aligned} \tag{4}$$

constrained by $\rho_{g_jg_j} + \rho_{r_jr_j} = 1$ and $\rho_{g_jr_j} = \rho^*_{r_jg_j}$ in the single-atom state basis of $|g_j\rangle$ and $|r_j\rangle$ and then calculate $\rho_{r_jr_j}$ with a certain initial condition. The reason is simply that a reduction from Eq. (3) to Eq. (4) will erase important contributions of the double-photon transition $|g_1g_2\rangle \to |r_1r_2\rangle$. In other words, the traced-out elements $\rho_{g_1r_1,g_2r_2}$ should have a significant influence on the dynamic evolutions of two interacting atoms.

The deviation degree of in-phase dynamics for a double Rydberg excitation can be measured by

$$D_{\rm in}(t) = \big|\rho_{r_2r_2}(t) - \rho_{r_1r_1}(t)\big|, \tag{5}$$

whose time-averaged value, as a figure of merit, should be calculated through the integral

$$\overline{D}_{\rm in} = \lim_{T\to\infty} \frac{1}{T}\int_{t=0}^{T} D_{\rm in}(t)dt, \tag{6}$$

with the optimal (worst) in-phase dynamics attained in the case of $\overline{D}_{\rm in} \to 0$ ($\overline{D}_{\rm in} \to 1$).

The deviation degree of antiphase dynamics for a double Rydberg excitation can be measured by

$$D_{\rm anti}(t) = \big|\big|\rho_{r_2r_2}(t) - 0.5\big| - \big|\rho_{r_1r_1}(t) - 0.5\big|\big|, \tag{7}$$

whose time-averaged value, as a figure of merit, should be calculated through the integral

$$\overline{D}_{\rm anti} = \lim_{T\to\infty} \frac{1}{T}\int_{t=0}^{T} D_{\rm anti}(t)dt, \tag{8}$$

with the optimal (worst) antiphase dynamics attained in the case of $\overline{D}_{\rm anti} \to 0$ ($\overline{D}_{\rm anti} \to 1$).

Now we consider two ^{87}Rb atoms with the Rydberg states $|r_1\rangle = |r_2\rangle = |90S, J = 1/2, m_J = 1/2\rangle$ and the ground states $|g_1\rangle = |5S_{1/2}, F = 2, m_F = -1\rangle$ and $|g_2\rangle = |5S_{1/2}, F = 2, m_F = 1\rangle$ as an example. Then it is easy to know $\Gamma_1 = \Gamma_2 \simeq 2.0$ kHz and $C_6 \simeq 2\pi \times 1.67 \times 10^{13}$ s$^{-1}\mu$m^6 [61,62], yielding thus a vdW potential in the range of $V_6 \in \{1 \leftrightarrow 60\}$ MHz for a distance in the range of $R_{12} \in \{8 \leftrightarrow 16\}$ μm. We further argue that our proposal could be realized in a three-level model by introducing the middle states $|e_1\rangle = |e_2\rangle = |5P_{1/2}, F = 1, m_F = 0\rangle$. An equivalent two-level model can be attained by adiabatically eliminating $|e_1\rangle$ and $|e_2\rangle$ in the case of very small two-photon detunings and very large single-photon detunings [60]. For this equivalent two-level model, the difference between detunings Δ_1 and Δ_2 can be easily tuned by an inhomogeneous magnetic field with the Zeeman effect. Note also that (i) a linearly polarized laser field can be applied to generate left and right circularly polarized components of identical amplitudes and (ii) the $|g_1\rangle \to |e_1\rangle$ and $|g_2\rangle \to |e_2\rangle$ transitions share the same electric dipole moments $d_{e_1g_1} = d_{e_2g_2}$ [63]. In this case, it is reasonable to set $\Omega_1 = \Omega_2 = \Omega$ and use Ω ($1/\Omega$) as the frequency (time) scale in what follows.

III. IN-PHASE DYNAMICS

In this section, we study via numerical calculations under what conditions and to what extent the two Rydberg atoms can exhibit the in-phase dynamics. This is done by first plotting in Fig. 2 in-phase deviation degree $\overline{D}_{\rm in}$ against vdW potential V_6 and initial population $\rho_{g_2g_2}(0)$ with $\rho_{g_1g_1}(0) = 1$, $\Delta_1/\Omega = 0.2$, and $\Delta_2/\Omega = 0.7$. It is clear that a larger difference in the initial ground populations typically results in a larger deviation degree of the in-phase dynamics except V_6 is close to zero. It is of particular interest that a vanishing deviation degree only appears at a specific point defined by $\rho_{g_2g_2}(0) = 1$ and $V_6/\Omega = 0.6$. As detunings Δ_1 and Δ_2 are changed, this specific point of $\overline{D}_{\rm in} \to 0$ is found to simply move along the V_6 axis with $\rho_{g_2g_2}(0) \equiv 1$ (not shown).

We then plot in Fig. 3 single-atom Rydberg populations $\rho_{r_ir_i}(t)$ and in-phase deviation degree $D_{\rm in}(t)$ against time t with initial condition $\rho_{g_1g_1,g_2g_2}(0) = 1$, for a few typical values of vdW potential V_6. Figures 3(a_1) and 3(a_2) show that the two Rydberg atoms oscillate independently with different periods due to $\Delta_1 \neq \Delta_2$, in the case of a vanishing vdW interaction. For a weak vdW interaction, we find from Figs. 3(b_1) and 3(b_2) that the two Rydberg atoms still oscillate out of phase, though they have been mutually coupled to result in additional beating-like oscillations. It is of particular interest to note from Figs. 3(c_1) and 3(c_2) that the two Rydberg atoms exhibit pretty good in-phase oscillations, as the vdW potential has a moderate value. For a strong vdW interaction,

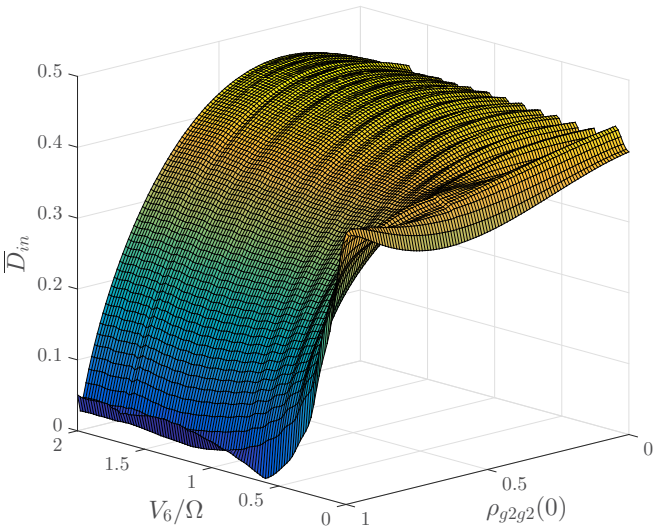

FIG. 2. Deviation degree $\overline{D}_{\rm in}$ against vdW potential V_6 and initial population $\rho_{g_2g_2}(0)$ with $\rho_{g_1g_1}(0) = 1$, $\Delta_1/\Omega = 0.2$, $\Delta_2/\Omega = 0.7$, and $\Gamma_1/\Omega = \Gamma_2/\Omega = 0.0002$.

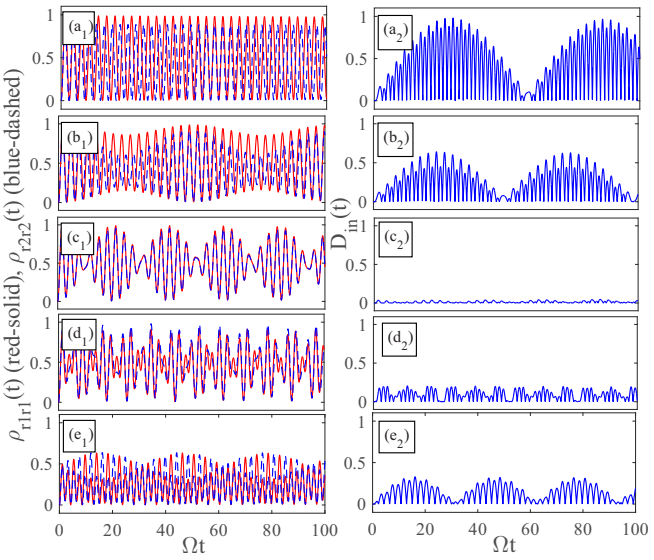

FIG. 3. Dynamic evolutions of Rydberg populations $\rho_{r_ir_i}(t)$ (left) and deviation degree $D_{\text{in}}(t)$ (right) with $V_6/\Omega = 0.0$ (a_1, a_2); $V_6/\Omega = 0.2$ (b_1, b_2); $V_6/\Omega = 0.6$ (c_1, c_2); $V_6/\Omega = 1.5$ (d_1, d_2); $V_6/\Omega = 10$ (e_1, e_2). Other parameters are the same as in Fig. 2 except $\rho_{g_1g_1,g_2g_2}(0) = 1$.

we find from Figs. 3(d_1) and 3(d_2) that the in-phase evolutions are somewhat destroyed with revived fluctuations in the deviation degree. As the vdW interaction is sufficiently strong, Figs. 3(e_1) and 3(e_2) display quite peculiar evolution dynamics: the maximal oscillation amplitudes are suppressed to ∼0.5 as a manifestation of the dipole blockade effect; the two Rydberg populations, though of same periods, are not in-phase because they exhibit alternatively enhanced and reduced amplitudes.

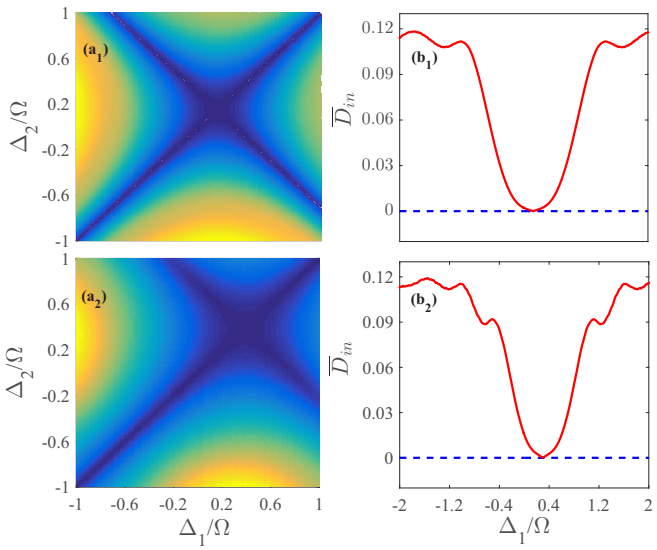

FIG. 4. $\overline{D}_{\text{in}}$ against Δ_1/Ω and Δ_2/Ω with $V_6/\Omega = 0.2$ (a_1); $V_6/\Omega = 0.4$ (a_2). The two curves in (b_1) and (b_2) are respectively extracted from (a_1) and (a_2) to compare the cases of $\Delta_1 = \Delta_2$ (blue-dashed) and $\Delta_1 + \Delta_2 = 3V_6/2$ (red-solid). Other parameters are the same as in Fig. 2.

General conditions for observing the in-phase dynamics can be found by plotting $\overline{D}_{\text{in}}$ against Δ_1 and Δ_2 for two different values of V_6 in Figs. 4(a_1) and 4(a_2). It is easy to conclude from a series of such plots that there always exist two intersecting dark lines accounting for the minimal in-phase deviation degree: a *trivial* one corresponding to $\Delta_1 = \Delta_2$ and a *nontrivial* one corresponding to $\Delta_1 + \Delta_2 = 3V_6/2$. Figures 4($b_1$) and 4($b_2$) further show that $\overline{D}_{\text{in}}$ (i) remains vanishing along the *trivial* dark line, indicating the *exact* in-phase dynamics; (ii) exhibits a smooth window along the *nontrivial* dark line, indicating the *approximate* in-phase dynamics. This in-phase window is centered at $\Delta_1 = \Delta_2 = 3V_6/4$ with its width depending somewhat on V_6. To be more specific, pretty good in-phase dynamics (e.g., with $\overline{D}_{\text{in}} \lesssim 0.05$) can be attained in the range $|\Delta_1 - \Delta_2|/\Omega \lesssim 0.65$ ($|\Delta_1 - \Delta_2|/\Omega \lesssim 0.50$) for $V_6/\Omega = 0.2$ ($V_6/\Omega = 0.4$).

IV. ANTIPHASE DYNAMICS

Now we turn to examine antiphase dynamics in a way similar to that used in the last section. We first plot in Fig. 5 antiphase deviation degree $\overline{D}_{\text{anti}}$ against vdW potential V_6 and initial population $\rho_{g_2g_2}(0)$, with the same parameters as in Fig. 2. We find that $\overline{D}_{\text{anti}}$ in Fig. 5 exhibits different behaviors as compared to $\overline{D}_{\text{in}}$ in Fig. 2. For instance, it is a smaller difference in the initial ground populations that results in a larger deviation degree of the antiphase dynamics except V_6 is close to zero. In addition, a vanishing deviation degree appears instead at the specific point defined by $\rho_{g_2g_2}(0) = 0$ and $V_6/\Omega = 0.9$. Of course, the specific point of $\overline{D}_{\text{anti}} \to 0$ will move along the V_6 axis with $\rho_{g_2g_2}(0) \equiv 0$, as detunings Δ_1 and Δ_2 are changed (not shown).

We then plot in Fig. 6 single-atom Rydberg populations $\rho_{r_ir_i}(t)$ and antiphase deviation degree $D_{\text{anti}}(t)$ against time t with initial condition $\rho_{g_1g_1,r_2r_2}(0) = 1$, for a few typical values of vdW potential V_6. Figures 6(a_1) and 6(a_2) show that the two Rydberg atoms oscillate independently with large fluctuations in the deviation degree due to $\Delta_1 \neq \Delta_2$, as the

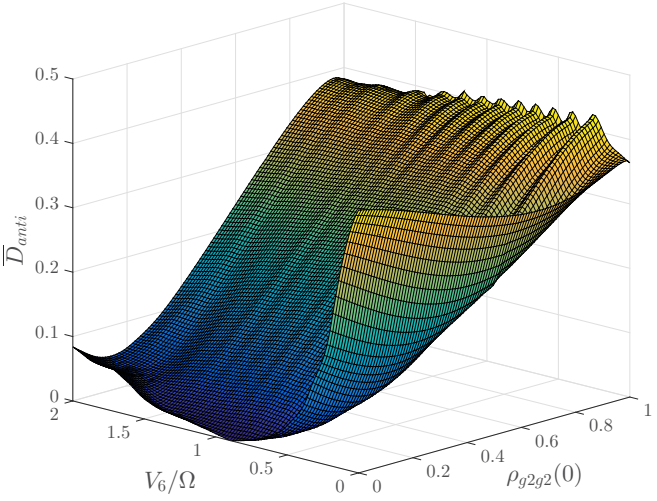

FIG. 5. Deviation degree $\overline{D}_{\text{anti}}$ against vdW potential V_6 and initial population $\rho_{g_2g_2}(0)$ with $\rho_{g_1g_1}(0) = 1$, $\Delta_1/\Omega = 0.2$, $\Delta_2/\Omega = 0.7$, and $\Gamma_1/\Omega = \Gamma_2/\Omega = 0.0002$.

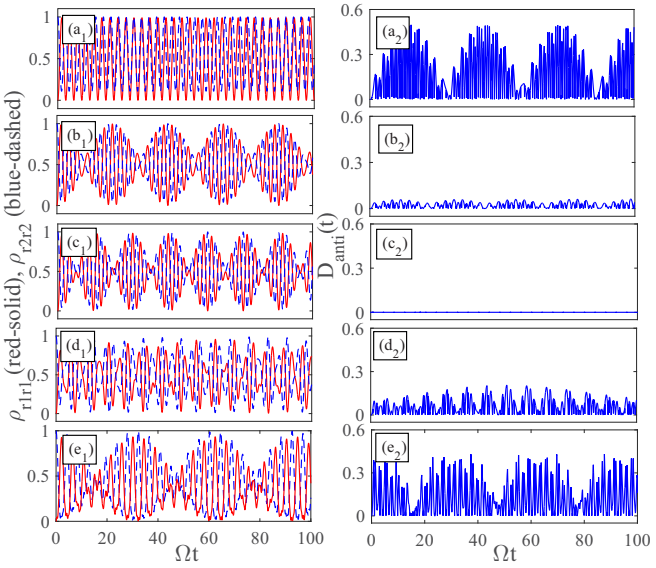

FIG. 6. Dynamic evolutions of Rydberg populations $\rho_{r_i r_i}(t)$ (left) and deviation degree $D_{\text{anti}}(t)$ (right) with $V_6/\Omega = 0.0$ (a_1, a_2); $V_6/\Omega = 0.6$ (b_1, b_2); $V_6/\Omega = 0.9$ (c_1, c_2); $V_6/\Omega = 1.8$ (d_1, d_2); $V_6/\Omega = 10$ (e_1, e_2). Other parameters are the same as in Fig. 5 except $\rho_{g_1g_1,r_2r_2}(0) = 1$.

vdW interaction is vanishing. For a weak vdW interaction, we find from Figs. 6(b_1) and 6(b_2) that the two Rydberg atoms become mutually coupled to result in additional beating-like oscillations with greatly suppressed fluctuations in the deviation degree. It is surprising to find from Figs. 6(c_1) and 6(c_2) that the two Rydberg atoms exhibit the *exact* antiphase oscillations because V_6 has a moderate value. For a strong vdW interaction, Figs. 6(d_1) and 6(d_2) show that the antiphase evolutions are obviously destroyed with revived fluctuations in the deviation degree. Since the vdW interaction is sufficiently strong, Figs. 6(e_1) and 6(e_2) display quite peculiar evolution dynamics: $\rho_{r_1r_1}(t)$ and $\rho_{r_2r_2}(t)$ are not antiphase, though exhibiting alternatively enhanced and reduced amplitudes in most time, with their sum $\lesssim 1.0$ as a manifestation of the dipole blockade effect.

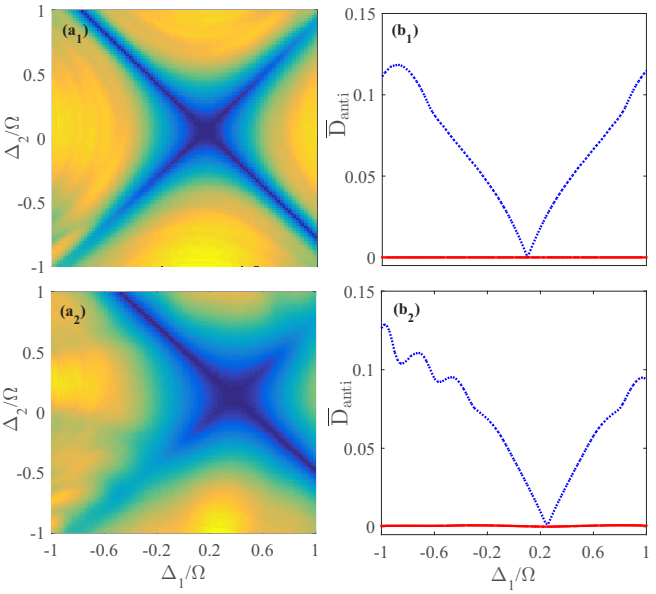

FIG. 7. $\overline{D}_{\text{anti}}$ against Δ_1/Ω and Δ_2/Ω with $V_6/\Omega = 0.2$ (a_1); $V_6/\Omega = 0.5$ (a_2). The two curves in (b_1) and (b_2) are respectively extracted from (a_1) and (a_2) to compare the cases of $\Delta_1 - \Delta_2 = V_6/2$ (blue-dashed) and $\Delta_1 + \Delta_2 = V_6$ (red-solid). Other parameters are the same as in Fig. 5.

General conditions for attaining the antiphase dynamics can be found by plotting $\overline{D}_{\text{anti}}$ against Δ_1 and Δ_2 for two different values of V_6 in Figs. 7(a_1) and 7(a_2). It is easy to conclude from a series of such plots that there always exist two intersecting dark lines accounting for the minimal antiphase deviation degree, which correspond respectively to $\Delta_1 - \Delta_2 = V_6/2$ and $\Delta_1 + \Delta_2 = V_6$ and therefore are both *nontrivial*. Figures 7(b_1) and 7(b_2) further show that $\overline{D}_{\text{anti}}$ (i) remains vanishing along the line determined by $\Delta_1 + \Delta_2 = V_6$, indicating the *exact* antiphase dynamics; (ii) exhibits a sharp window along the line determined by $\Delta_1 - \Delta_2 = V_6/2$, indicating the *approximate* antiphase dynamics. Comparing Figs. 4 and 7, we can say that the *nontrivial* antiphase dynamics could be *exact* while the *nontrivial* in-phase dynamics is always *approximate* for two interacting atoms with different driving detunings (resonant frequencies).

V. DISCUSSION

With regard to Fig. 8(a), we first discuss why the *exact* and *approximate* in-phase dynamics are observed along two intersecting dark lines in the space of Δ_1 and Δ_2. For two atoms initially prepared in $|g_1g_2\rangle$ or $|r_1r_2\rangle$, the in-phase dynamics requires that they have identical transition probabilities toward $|g_1r_2\rangle$ and $|r_1g_2\rangle$. Otherwise, $\rho_{g_1g_1,r_2r_2}$ and $\rho_{r_1r_1,g_2g_2}$ will become unbalanced so that it is impossible to have $\rho_{r_1r_1} = \rho_{r_2r_2}$. Intuitively, such identical transition probabilities can be attained when transitions $|g_1g_2\rangle \to |g_1r_2\rangle$ and $|g_1g_2\rangle \to |r_1g_2\rangle$ have the same or opposite detunings $\Delta_2 = \pm\Delta_1$ as well as transitions $|r_1r_2\rangle \to |g_1r_2\rangle$ and $|r_1r_2\rangle \to |r_1g_2\rangle$ have the same or opposite detunings $-(\Delta_1 - V_6) = \mp(\Delta_2 - V_6)$. Both conditions of the same detunings can be satisfied with $\Delta_1 = \Delta_2$, which then yields the *exact* in-phase dynamics. The two conditions of opposite detunings, however, result in contradicting requirements $\Delta_1 + \Delta_2 = 0$ and $\Delta_1 + \Delta_2 = 2V_6$

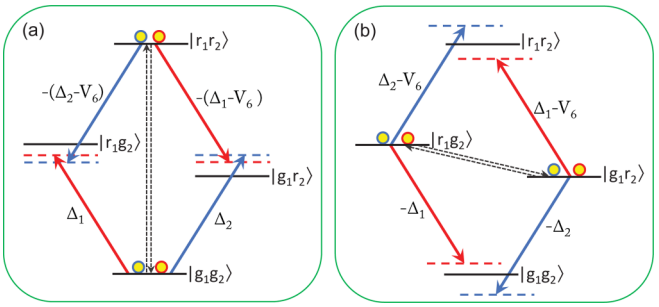

FIG. 8. (a) Relevant transitions for two atoms initially prepared in $|g_1g_2\rangle$ or $|r_1r_2\rangle$, which allows for the in-phase dynamics under appropriate conditions. (b) Relevant transitions for two atoms initially prepared in $|g_1r_2\rangle$ or $|r_1g_2\rangle$, which allows for the antiphase dynamics under appropriate conditions.

V. DISCUSSION

With regard to Fig. 8(a), we first discuss why the *exact* and *approximate* in-phase dynamics are observed along two intersecting dark lines in the space of Δ_1 and Δ_2. For two atoms initially prepared in $|g_1g_2\rangle$ or $|r_1r_2\rangle$, the in-phase dynamics requires that they have identical transition probabilities toward $|g_1r_2\rangle$ and $|r_1g_2\rangle$. Otherwise, $\rho_{g_1g_1,r_2r_2}$ and $\rho_{r_1r_1,g_2g_2}$ will become unbalanced so that it is impossible to have $\rho_{r_1r_1} = \rho_{r_2r_2}$. Intuitively, such identical transition probabilities can be attained when transitions $|g_1g_2\rangle \to |g_1r_2\rangle$ and $|g_1g_2\rangle \to |r_1g_2\rangle$ have the same or opposite detunings $\Delta_2 = \pm\Delta_1$ as well as transitions $|r_1r_2\rangle \to |g_1r_2\rangle$ and $|r_1r_2\rangle \to |r_1g_2\rangle$ have the same or opposite detunings $-(\Delta_1 - V_6) = \mp(\Delta_2 - V_6)$. Both conditions of the same detunings can be satisfied with $\Delta_1 = \Delta_2$, which then yields the *exact* in-phase dynamics. The two conditions of opposite detunings, however, result in contradicting requirements $\Delta_1 + \Delta_2 = 0$ and $\Delta_1 + \Delta_2 = 2V_6$

so that only the *approximate* antiphase dynamics can be observed along the line $\Delta_1 + \Delta_2 = 3V_6/2$. This can be regarded as an average of the three detunings from $|g_1g_2\rangle$ to $|g_1r_2\rangle$, $|r_1g_2\rangle$, and $|r_1r_2\rangle$.

Looking at Fig. 8(b), we now discuss why the *exact* and *approximate* antiphase dynamics are observed along two intersecting dark lines in the space of Δ_1 and Δ_2. For two atoms initially prepared in $|r_1g_2\rangle$ or $|g_1r_2\rangle$, the antiphase dynamics requires that they have equal transition probabilities toward $|g_1g_2\rangle$ and $|r_1r_2\rangle$. Otherwise, $\rho_{r_1r_1,r_2r_2}$ and $\rho_{g_1g_1,g_2g_2}$ will become unbalanced so that it is impossible to have $\rho_{r_1r_1} = \rho_{g_2g_2}$. Intuitively, such equal transition probabilities can be attained when transitions $|r_1g_2\rangle \to |g_1g_2\rangle$ and $|r_1g_2\rangle \to |r_1r_2\rangle$ have the same or opposite detunings $\Delta_2 - V_6 = \mp\Delta_1$ as well as transitions $|g_1r_2\rangle \to |g_1g_2\rangle$ and $|g_1r_2\rangle \to |r_1r_2\rangle$ have the same or opposite detunings $\Delta_1 - V_6 = \mp\Delta_2$. Both conditions of same detunings can be satisfied with $\Delta_1 + \Delta_2 = V_6$, which then yields the *exact* antiphase dynamics. The two conditions of opposite detunings, however, result in contradicting requirements $\Delta_1 - \Delta_2 = -V_6$ and $\Delta_1 - \Delta_2 = V_6$ so that only the *approximate* antiphase dynamics can be observed along the line $\Delta_1 - \Delta_2 = V_6/2$. This can be regarded as an average of the three detunings from $|g_1r_2\rangle$ to $|g_1g_2\rangle$, $|r_1r_2\rangle$, and $|r_1g_2\rangle$.

Finally, we note that a pair of closely lying Rydberg atoms can only be in the ground state $|gg\rangle$ and the symmetric state $(|gr\rangle + |rg\rangle)/\sqrt{2}$ but are forbidden to be in the asymmetric state $(|gr\rangle - |rg\rangle)/\sqrt{2}$ due to destructive interference and the double Rydberg state $|rr\rangle$ due to dipole blockade [60]. Thus, each Rydberg atom with states $|g\rangle$ and $|r\rangle$ in our model may be replaced by a pair of closely lying Rydberg atoms with states $|gg\rangle$ and $(|gr\rangle + |rg\rangle)/\sqrt{2}$. In this case, it is viable to have a reliable scheme for implementing the in-phase and antiphase dynamic control of atomic entanglement, when the two pairs of Rydberg atoms are spaced far enough to yield a moderate vdW potential ($V_6 \simeq \Omega$). In addition, we note from Ref. [60] that it is important to attain a high-fidelity Bell state $(|gr\rangle + |rg\rangle)/\sqrt{2}$ in the blockade regime. This Bell state [another Bell state $(|gg\rangle - |rr\rangle)/\sqrt{2}$] can also be attained, far from the blockade regime without requiring an infinitely large vdW potential ($V_6 \gg \Omega$), by exploring the antiphase (in-phase) dynamics in our model. The only requirement is to switch off the driving field at the beating nodes where $\rho_{r_1r_1} = \rho_{r_2r_2} = 0.5$ [see Figs. 3(c_1) and 6(c_1)]. Our alternative scheme for attaining these entangled states has two main advantages: (i) it works with a moderate and tunable vdW potential without needing to enter the blockade regime; (ii) it works in the presence of an inhomogeneous magnetic field without requiring the same atom-light detunings.

VI. CONCLUSIONS

In summary, we have studied a pair of two-level Rydberg atoms interacting via a vdW potential V_6 to examine their correlated dynamic evolutions. The two atoms can exhibit the *exact* or *approximate* in-phase dynamics, when they are both prepared in the ground states at the initial time. The *exact* ones are found to require $\Delta_1 = \Delta_2$ and deemed as *trivial* because they hold even for $V_6 = 0$. The *approximate* ones require instead $\Delta_1 + \Delta_2 = 3V_6/2$ and are therefore *nontrivial* because they hold only for $V_6 \neq 0$. In particular, the *approximate* one manifests as a narrow window in which deviation degree $\overline{D}_{\rm in}$ gradually increases as detuning difference $|\Delta_1 - \Delta_2|$ becomes larger. The two atoms may also exhibit the *exact* or *approximate* antiphase dynamics, when they are respectively prepared in the ground and Rydberg states at the initial time. The *exact* and *approximate* ones are both *nontrivial* because they require $\Delta_1 + \Delta_2 = V_6$ and $\Delta_1 - \Delta_2 = V_6/2$, respectively. In particular, the *exact* ones exist in a much wider range of Δ_1 and Δ_2 in which deviation degree $\overline{D}_{\rm anti}$ is vanishing, independent of detuning difference $|\Delta_1 - \Delta_2|$. Requirements for in-phase and antiphase dynamics can be understood by considering the balanced transitions from two initially populated states to two initially empty states in the double-atom state basis. Our results should be instructive in devising schemes of quantum manipulation on atomic entanglement, though they are not easily extended for more Rydberg atoms in the 1D chains or 2D arrays.

ACKNOWLEDGMENTS

J.-H.W. thanks S. Chesi, M. Artoni, and G. C. La Rocca for helpful discussions. The work is supported by the National Natural Science Foundation of China (No. 10534002 and No. 11674049) as well as the Cooperative Program by the Italian Ministry of Foreign Affairs & International Cooperation (No. PGR00960) and the National Natural Science Foundation of China (No. 11861131001).

[1] M. Saffman, T. G. Walker, and K. Mølmer, Rev. Mod. Phys. **82**, 2313 (2010).
[2] T. Vogt, M. Viteau, A. Chotia, J. M. Zhao, D. Comparat, and P. Pillet, Phys. Rev. Lett. **99**, 073002 (2007).
[3] M. D. Lukin, M. Fleischhauer, R. Cote, L. M. Duan, D. Jaksch, J. I. Cirac, and P. Zoller, Phys. Rev. Lett. **87**, 037901 (2001).
[4] C. Ates, T. Pohl, T. Pattard, and J. M. Rost, Phys. Rev. Lett. **98**, 023002 (2007).
[5] T. Amthor, C. Giese, C. S. Hofmann, and M. Weidemüller, Phys. Rev. Lett. **104**, 013001 (2010).
[6] J. T. Young, T. Boulier, E. Magnan, E. A. Goldschmidt, R. M. Wilson, S. L. Rolston, J. V. Porto, and A. V. Gorshkov, Phys. Rev. A **97**, 023424 (2018).
[7] R. G. Unanyan and M. Fleischhauer, Phys. Rev. A **66**, 032109 (2002).
[8] T. Wilk, A. Gaetan, C. Evellin, J. Wolters, Y. Miroshnychenko, P. Grangier, and A. Browaeys, Phys. Rev. Lett. **104**, 010502 (2010).
[9] D. Yan, C.-L. Cui, M. Zhang, and J.-H. Wu, Phys. Rev. A **84**, 043405 (2011).
[10] F. Bariani, Y. O. Dudin, T. A. B. Kennedy, and A. Kuzmich, Phys. Rev. Lett. **108**, 030501 (2012).
[11] D. D. Bhaktavatsala Rao and K. Mølmer, Phys. Rev. Lett. **111**, 033606 (2013).
[12] E. Brion, K. Molmer, and M. Saffman, Phys. Rev. Lett. **99**, 260501 (2007).

[13] D. Moller, L. B. Madsen, and K. Molmer, Phys. Rev. Lett. **100**, 170504 (2008).

[14] L. Isenhower, E. Urban, X.-L. Zhang, A. T. Gill, T. Henage, T. A. Johnson, T. G. Walker, and M. Saffman, Phys. Rev. Lett. **104**, 010503 (2010).

[15] M. H. Goerz, E. J. Halperin, J. M. Aytac, C. P. Koch, and K. B. Whaley, Phys. Rev. A **90**, 032329 (2014).

[16] X.-Q. Shao, J.-H. Wu, and X.-X. Yi, Phys. Rev. A **95**, 062339 (2017).

[17] S. Baur, D. Tiarks, G. Rempe, and S. Durr, Phys. Rev. Lett. **112**, 073901 (2014).

[18] W. Li and I. Lesanovsky, Phys. Rev. A **92**, 043828 (2015).

[19] H. Gorniaczyk, C. Tresp, J. Schmidt, H. Fedder, and S. Hofferberth, Phys. Rev. Lett. **113**, 053601 (2014).

[20] D. Tiarks, S. Baur, K. Schneider, S. Durr, and G. Rempe, Phys. Rev. Lett. **113**, 053602 (2014).

[21] Y.-M. Liu, X.-D. Tian, X. Wang, D. Yan, and J.-H. Wu, Opt. Lett. **41**, 408 (2016).

[22] M. Saffman and T. G. Walker, Phys. Rev. A **66**, 065403 (2002).

[23] M. M. Muller, A. Kolle, R. Low, T. Pfau, T. Calarco, and S. Montangero, Phys. Rev. A **87**, 053412 (2013).

[24] J. L. Miller, Phys. Today **65**(7), 14 (2012).

[25] D. Petrosyan and K. Molmer, Phys. Rev. Lett. **121**, 123605 (2018).

[26] J. D. Pritchard, D. Maxwell, A. Gauguet, K. J. Weatherill, M. P. A. Jones, and C. S. Adams, Phys. Rev. Lett. **105**, 193603 (2010).

[27] C. Ates, S. Sevincli, and T. Pohl, Phys. Rev. A **83**, 041802 (2011).

[28] D. Petrosyan, J. Otterbach, and M. Fleischhauer, Phys. Rev. Lett. **107**, 213601 (2011).

[29] Y.-M. Liu, D. Yan, X.-D. Tian, C.-L. Cui, and J.-H. Wu, Phys. Rev. A **89**, 033839 (2014).

[30] A. V. Gorshkov, J. Otterbach, M. Fleischhauer, T. Pohl, and M. D. Lukin, Phys. Rev. Lett. **107**, 133602 (2011).

[31] T. Caneva, M. T. Manzoni, T. Shi, J. S. Douglas, J. I. Cirac, and D. E. Chang, New J. Phys. **17**, 113001 (2015).

[32] L. Yang, B. He, J.-H. Wu, Z.-Y. Zhang, and M. Xiao, Optica **3**, 1095 (2016).

[33] M. J. Gullans, J. D. Thompson, Y. Wang, Q.-Y. Liang, V. Vuletic, M. D. Lukin, and A. V. Gorshkov, Phys. Rev. Lett. **117**, 113601 (2016).

[34] O. Firstenberg, T. Peyronel, Q.-Y. Liang, A. V. Gorshkov, M. D. Lukin, and V. Vuletic, Nature **502**, 71 (2013).

[35] M. F. Maghrebi, M. J. Gullans, P. Bienias, S. Choi, I. Martin, O. Firstenberg, M. D. Lukin, H. P. Buchler, and A. V. Gorshkov, Phys. Rev. Lett. **115**, 123601 (2015).

[36] K. Jachymski, P. Bienias, and H. P. Buchler, Phys. Rev. Lett. **117**, 053601 (2016).

[37] Q. Y. Liang, A. V. Venkatramani, S. H. Cantu, T. L. Nicholson, M. J. Gullans, A. V. Gorshkov, J. D. Thompson, C. Chin, M. D. Lukin, and V. Vuletic, Science **359**, 783 (2018).

[38] D. Paredes-Barato and C. S. Adams, Phys. Rev. Lett. **112**, 040501 (2014).

[39] M. Khazali, K. Heshami, and C. Simon, Phys. Rev. A **91**, 030301 (2015).

[40] J.-H. Wu, M. Artoni, F. Cataliotti, and G. C. La Rocca, Europhys. Lett. **120**, 54002 (2017).

[41] E. Distante, A. Padron-Brito, M. Cristiani, D. Paredes-Barato, and H. de Riedmatten, Phys. Rev. Lett. **117**, 113001 (2016).

[42] E. Distante, P. Farrera, A. Padron-Brito, D. Paredes-Barato, G. Heinze, and H. de Riedmatten, Nat. Commun. **8**, 14072 (2017).

[43] X.-D. Tian, Y.-M. Liu, Q.-Q. Bao, J.-H. Wu, M. Artoni, and G. C. La Rocca, Phys. Rev. A **97**, 043811 (2018).

[44] S.-L. Su, Y. Gao, E.-J. Liang, and S. Zhang, Phys. Rev. A **95**, 022319 (2017).

[45] H.-Z. Wu, X.-R. Huang, C.-S. Hu, Z.-B. Yang, and S.-B. Zheng, Phys. Rev. A **96**, 022321 (2017).

[46] D. Petrosyan, F. Motzoi, M. Saffman, and K. Molmer, Phys. Rev. A **96**, 042306 (2017).

[47] Y. Zeng, P. Xu, X. D. He, Y. Y. Liu, M. Liu, J. Wang, D. J. Papoular, G. V. Shlyapnikov, and M. S. Zhan, Phys. Rev. Lett. **119**, 160502 (2017).

[48] I. I. Beterov, I. N. Ashkarin, E. A. Yakshina, D. B. Tretyakov, V. M. Entin, I. I. Ryabtsev, P. Cheinet, P. Pillet, and M. Saffman, Phys. Rev. A **98**, 042704 (2018).

[49] X.-F. Shi, Phys. Rev. Appl. **9**, 051001 (2018).

[50] C. Ates, A. Eisfeld, and J. M. Rost, New J. Phys **10**, 045030 (2008).

[51] S. Wuster, C. Ates, A. Eisfeld, and J. M. Rost, Phys. Rev. Lett. **105**, 053004 (2010).

[52] D. Barredo, H. Labuhn, S. Ravets, T. Lahaye, A. Browaeys, and C. S. Adams, Phys. Rev. Lett. **114**, 113002 (2015).

[53] H. Schempp, G. Gunter, S. Wuster, M. Weidemuller, and S. Whitlock, Phys. Rev. Lett. **115**, 093002 (2015).

[54] T. E. Lee, H. Haffner, and M. C. Cross, Phys. Rev. A **84**, 031402 (2011).

[55] J. Zeiher, J. Y. Choi, A. Rubio-Abadal, T. Pohl, R. van Bijnen, I. Bloch, and C. Gross, Phys. Rev. X **7**, 041063 (2017).

[56] H. Labuhn, D. Barredo, S. Ravets, S. de Leseleuc, T. Macri, T. Lahaye, and A. Browaeys, Nature **534**, 667 (2016).

[57] J. Gillet, G. S. Agarwal, and T. Bastin, Phys. Rev. A **81**, 013837 (2010).

[58] J. Qian, L. Zhang, J.-J. Zhai, and W.-P. Zhang, Phys. Rev. A **92**, 063407 (2015).

[59] V. R. Overbeck and H. Weimer, Phys. Rev. A **93**, 012106 (2016).

[60] H. Levine, A. Keesling, A. Omran, H. Bernien, S. Schwartz, A. S. Zibrov, M. Endres, M. Greiner, V. Vuletic, and M. D. Lukin, Phys. Rev. Lett. **121**, 123603 (2018).

[61] K. Singer, J. Stanojevic, M. Weidemuller, and R. Cote, J. Phys. B: At. Mol. Opt. **38**, S295 (2005).

[62] J.-H. Wu, M. Artoni, and G. C. La Rocca, Phys. Rev. A **92**, 063805 (2015).

[63] https://steck.us/alkalidata/.